Nanomed Res J 9(3):298-307, Summer 2024

RESEARCH ARTICLE

Compression of radio and photo sensitivity of 5-aminolevulinic acid (5-ALA) conjugated hollow gold nanoparticles (HGNs) on KYSE cell line of oesophageal cancer

Zahra Mohammadi[1], Armin Imanparast[2], Hoda Talebian[3], Nafiseh Sobhani[4], Maryam Shabanzadeh[5], Ameneh Sazgarnia[2*]

[1] Radiological Technology Department of Faculty Paramedical Sciences, Babol University of Medical Sciences, Babol, Iran

[2] Medical Physics Research Center, Faculty of Medicine, Mashhad University of Medical Sciences, Mashhad, Iran

[3] Department of Medical Physics Radiobiology and Radiation Protection, School of Medicine, Babol University of Medical Sciences, Babol, Iran

[4] PhD Candidate of Neuroimaging at the Tehran University of Medical Sciences, Tehran, Iran

[5] Islamic Azad University Science and Research Branch, Tehran, Iran

ARTICLE INFO

Article History:
Received 03 Jun 2024
Accepted 28 Jul 2024
Published 01 Aug 2024

Keywords:
Hollow gold nanoparticles (HGNs)
5-aminolevulinic acid
Radiotherapy
PDT
oesophageal cancer

ABSTRACT

Objective(s): Nanoparticles can be used in therapies by increasing drug delivery and radiosensitivity. In this study, we investigated the radio- and photo-sensitivity of the conjugation of 5-aminolevulinic acid (5-ALA) and hollow gold nanoparticles (conjugate) on the KYSE cells.

Methods: After the determination of the dark toxicity of the therapeutic agent, the experiments were performed at three different radiation doses. Then, the photodynamic effect of each of group was analyzed at three optical doses.

Results: There was no significant difference between the control and treatment groups in X-ray treatment. In the photodynamic therapy (PDT), a significant difference was noted between the control group and the treatment groups, particularly within the 5-ALA and conjugate groups. Notably, the conjugate group induced approximately 90% cell death.

Conclusions: The study found that the conjugate induced a cell death rate more than three times higher than that of free 5-ALA alone. Thus, it can be concluded that the conjugate serves as an effective delivery agent for 5-ALA and enhances tumor cell destruction following PDT.

How to cite this article
Mohammadi Z., Imanparast A., Talebian H., Sobhani N., Shabanzadeh M., Sazgarnia A. Compression of radio and photo sensitivity of 5-aminolevulinic acid (5-ALA) conjugated hollow gold nanoparticles (HGNs) on KYSE cell line of oesophageal cancer. Nanomed Res J, 2024; 9(3): 298-307. DOI: 10.22034/nmrj.2024.03.007

INTRODUCTION

Radiotherapy (RT) is a key treatment for various cancers, showing significant advancements in patient management and symptom relief. Esophageal squamous cell carcinoma (ESCC) is a serious global health issue, being the sixth leading cause of cancer-related deaths. While esophagectomy or chemoradiotherapy (CRT) is standard for cancers with submucosal invasion, RT or CRT alone is often recommended for elderly patients to preserve organ function and improve quality of life (1). Despite significant progress in cancer treatments, challenges remain, including damage to healthy tissues, the spread of cancer (metastasis), the growth of new blood vessels to support tumors (angiogenesis), alterations in metabolism, and the recurrence of the disease(2). In adjuvant strategies for RT, photodynamic therapy (PDT) has emerged as a promising, minimally

* Corresponding Author Email: *sazgarniaa@mums.ac.ir*

invasive approach. It is particularly beneficial for patients in early cancer stages who cannot undergo surgery or in cases of local recurrence following initial treatment (3, 4). PDT offers minimal tissue toxicity and limited systemic effects, which significantly reduce long-term morbidity when used in multimodal cancer treatment approaches. (3, 4). PDT directly destroys tumor cells through apoptosis and/or necrosis, while also disrupting tumor vasculature and inducing inflammatory responses. This occurs following exposure to a photosensitizer (PS) and the formation of singlet oxygen (5). There are three groups of photosensitizers (PSs) used in PDT. Photofrin, the first FDA-approved PS in 1995, is utilized for treating esophageal and non-small cell lung cancer. However, it has side effects, particularly prolonged photosensitivity of the eyes and skin for up to six weeks after treatment, requiring patients to avoid sunlight and certain indoor lighting. The second generation of photosensitizers, designed with improved chemical properties, includes various compounds such as chlorins, purpurins, porphyrins, pheophorbides, phthalocyanines, bacteriopheophorbides, metalloporphyrins, and boronated porphyrins (BOPP). 5-aminolevulinic acid (5-ALA) is another important component in the second generation of photosensitizers. Acting as a precursor to protoporphyrin IX (PpIX), 5-ALA is administered and selectively absorbed by tumor vasculature. It then undergoes a series of cellular and enzymatic transformations, ultimately converting into the active PpIX photosensitizer. This process enhances its effectiveness, making 5-ALA a key element in advanced PDT applications (6). The in situ administration of 5-ALA and the rapid clearance of the resulting Protoporphyrin IX (PpIX) help minimize unwanted optical side effects (7). Advancements in nanotechnology, and drug delivery systems have enhanced tumor targeting in the development and application of third-generation photosensitizers (8-10). To improve targeted delivery of photosensitizers (PS) to tumors, challenges such as low lipid solubility, limited cell membrane passage, and tumor tissue's leaky vasculature must be addressed. Nanocarriers have been proposed as effective solutions, leveraging the enhanced permeation and retention (EPR) effect to promote selective accumulation of photosensitizing agents in tumor cells (11, 12). Gold nanoparticles have gained significant attention in fields like imaging, immunoassays, drug delivery, and PDT due to their ease of synthesis, biocompatibility, and exceptional optical and surface plasmon resonance (SPR) properties. These unique characteristics make gold nanoparticles highly valuable for advancing research and applications, driving substantial interest among scientists and professionals. (12, 13) . Nanoscale structures offer a high surface area relative to their size, making them ideal for loading, conjugating, and binding therapeutic agents, leading to more efficient targeted therapies, improved drug solubility, and enhanced stability (12). Hollow gold nanoparticles (HGNs) are particularly advantageous due to their elevated localized surface plasmon resonance (LSPR) and superior photothermal conversion compared to solid gold nanoparticles. This is attributed to their two-interface structure and the coupling of plasmon modes between the inner and outer surfaces. (14). HGNs possess notable properties such as photodegradation stability, tuneable near-infrared (NIR) absorption (520-1000nm), biocompatibility, and a high surface-to-volume ratio. These characteristics have been explored in various studies (14, 15). Additionally, HGNs can enhance the effectiveness of sensitizers as ideal radio amplifiers, benefiting from advanced surface coating techniques and dynamic properties (16). This study investigated the radio- and photo-sensitivity of a conjugated form of 5-ALA and HGNs during RT and PDT using the KYSE esophageal cancer cell line.

METHODS AND MATERIAL

Trisodium citrate dihydrate (>99%), cobalt chloride hexahydrate (99.99%), penicillin, Trypan blue, chloroauric acid ($HAuCl_4 \cdot 4H_2O$), trisodium citrate dihydrate (>99%), 5-ALA (95%), RPMI 1640, streptomycin, and sodium borohydride (99%) were purchased from Sigma-Aldrich (St. Louis, MO, USA). Fetal bovine serum (FBS) was provided by the Gibco company (USA, lot number 371748). To detach cells from the vessel's surface, EDTA trypsin from the Biogen Organization (Iran) and MTT (3-4,5-dimethylthiazol-2-yl-2,5-diphenyltetrazolium bromide) powder were purchased from Merck Company to be used for assessing cell survival in this study.

Synthesis of HGNS and PEGylation (Polyethylene glycol) and conjugating with 5-ALA

The synthesis process of HGNs optimized in the previous study requires the use of sterile ultrapure

water that must be deoxygenated with nitrogen or argon gas before synthesis. Additionally, all tools used throughout the synthesis process must be autoclaved to maintain sterility. The synthesis of HGNs begins with the production of oxygen-sensitive cobalt nanoparticles (OSCNs), followed by the deposition of a gold shell over them. The hollow gold shell is then obtained by oxidizing the cobalt core. For this process, 120 µl of 0.1 M sodium citrate and 30 µl of 1 M sodium tetrahydroborate are mixed in 30 ml of oxygen-free ultrapure water. Following the addition of 30 µl of 0.4 M cobalt chloride, an opaque brown compound forms, indicating the production of oxygen-sensitive cobalt nanoparticles (OSCNs). The processing time is influenced by the initial temperature of the water. The synthesis of oxygen-sensitive cobalt nanoparticles (OSCNs) occurs more quickly at higher temperatures. After synthesis, the OSCNs were mixed with 10 mL of oxygen-free ultrapure water and 25 mL of 0.1 M chloroauric acid using a vortex apparatus. This reaction resulted in the formation of a gold shell around the cobalt nanoparticles. To create hollow gold nanoshells, the solution was exposed to oxygen, oxidizing the cobalt core. A color change from dark brown to green signified the oxidation of OSCNs and the formation of the hollow gold nanoshells (GN1).

Characterization of nanostructures

Size distribution analysis

The nanoparticle size distribution was measured using a dynamic light scattering (DLS) particle size analyzer (DLS) (Zetasizer Nano ZS, Malvern, UK).

UV–Vis spectrophotometry

UV-vis absorption spectra were recorded at room temperature using a UNICO UV-2100 spectrophotometer (USA) equipped with 1.0 cm quartz cells.

Transmission electron microscopy (TEM)

Transmission electron microscopy (TEM) was used to examine the morphology and size distribution of the synthesized particles. The analysis was conducted using a Philips CM 120 TEM, operated at 100 kV.

Fourier Transform Infrared Spectroscopy (FTIR)

FTIR analysis was conducted using the AVATAR 370 FT-IR Nicolet T system (USA) to qualitatively and quantitatively identify organic compounds associated with the nanoparticles. This analysis also helped determine the types of functional groups and bonds present in the molecules.

In-Vitro Study

cell culture conditions

This study utilized a cell line derived from patients with malignant melanoma, a form of skin cancer, obtained from melanoma units in urban centers and Sydney, Australia. [27]. The cells were cultured as a monolayer in 75 cm² plastic tissue culture flasks containing RPMI 1640 medium, supplemented with 10% FBS and 1% antibiotics (penicillin at 50 U/ml and streptomycin at 50 mg/ml). The cells were incubated at 37°C in a humidified atmosphere with elevated CO_2 levels. Once confluence was reached, the cells were detached from the flask surface using EDTA. Prior to treatment, cell counting and viability assessment, which showed over 98% viability, were conducted using Trypan blue staining.

Cytotoxicity of 5-ALA, HGNs, and the conjugate

This section of the study aimed to identify the optimal non-toxic concentration of 5-ALA for the KYSE 30 cell line, with no treatments applied during this phase. Initially, 10^4 KYSE 30 cells were seeded into each well of a 96-well plate and incubated for 24 hours in a humidified incubator at 37°C. RPMI 1640 cell culture medium, supplemented with 1% penicillin/streptomycin, was used. Subsequently, the cells were washed with phosphate-buffered saline (PBS) and then incubated with varying concentrations of 5-ALA for a 4-hour period. Cell viability was evaluated using the MTT assay, and the results were obtained using an ELISA reader (AWERNESS Company, FAX 2100, USA) at a wavelength of 545 nm in the 96-well plates. The dark toxicity of 5-ALA was evaluated at concentrations of 0.25, 0.5, 1, 2, and 4 mM, while the dark toxicity of HGNs was assessed at concentrations of 0.05, 0.1, 0.2, and 0.4 mM. Finally, the cytotoxicity of the conjugate was assessed at concentrations of 0.5, 1, and 3 mM of 5-ALA. Each test group was repeated three times for robust analysis.

Investigation of radiotoxicity in the in-vitro environment

The study involved treating KYSE 30 cells

with various protocols to assess the effects of radiation and other compounds. After confirming cell viability, the protocols included: (1) a control group to compare radiation effects, (2) examining radiation effects in the presence of 5-ALA, (3) evaluating the growth of HAuNPs under radiation at different doses, and (4) studying the influence of conjugates combined with varying radiation doses. Each step focused on understanding how these treatments affect the cells under different radiation conditions. Cell concentrations were standardized, and after incubation, the cells were irradiated using a surface X-ray tube (Philips, 100 kVp). To promote cell proliferation post-irradiation, specific culture medium supplements were added and incubated. All experiments were conducted in triplicate to ensure rigorous and consistent evaluation across the different treatment groups.

Investigation of PDT in the in-vitro environment

After determining the optimal concentrations of 5-ALA, HGNs, and the conjugate in the previous section, the cells were irradiated using a He-Ne laser (628 nm, 220 V, 50 Hz, Atomic Energy Research Center, Iran) (1, 3, and 5 minutes at 80 J/cm² optical density). Following the addition of 100 mL of RPMI 1640 supplemented with 10% FBS to the wells and a 24-hour incubation, the evaluation of treatment efficacy was conducted by dividing KYSE cells into four distinct experimental groups.: (1) control, (2) groups treated with 5-ALA, (3) HGNs, and (4) conjugated nanoparticles by varying light doses.

Cell Survival Assay

Cell viability was evaluated using the MTT assay. In each well, 10 µl of MTT solution (0.5 mg/ml) was added, and the plate was covered with aluminum foil to protect from light exposure, which could interfere with MTT reduction. After a 4-hour incubation period, the plates were replenished with 200 µl of dimethyl sulfoxide (DMSO) to dissolve the formazan crystals produced by MTT reduction. The absorbance of the resulting solution was obtained at 545 nm using a 96-well ELISA reader (Awareness, Model STATFAX 2100, USA). This procedure was repeated three times to ensure the accuracy and precision of the results.

Statistical analysis

The normality of the data was verified using the Kolmogorov-Smirnov test. Statistical analysis was performed using one-way ANOVA, followed by the Tukey post-hoc test, with the SPSS software package (version 16).

RESULTS

Characterization

Particle size distribution, zeta potential, and polydispersity index (PDI) of HGNs

HGNs were synthesized with an average size of approximately 43 nm, as determined by dynamic light scattering (DLS) analysis. Table. 1 shows the size, zeta-potential, PDI, and conductivity of **HGNs** and **HGNs-PEG**.

TEM of HGNs

Figure 1 shows a TEM image of synthesized HGNs exhibiting a surface plasmon resonance band in the visible to infrared range, varying with the shell thickness to core ratio.

Fourier Transform Infrared Spectroscopy (FTIR)

FTIR is regarded as one of the most effective methods to detect the presence of different functional groups and to investigate the chemical composition of the surface in the process of conjugating different pharmaceutical agents to the surface of nanomaterials. Figure 2 shows the FTIR of conjugated 5-ALA to HGNs. The main peak was obtained at 843, 962, 1109, and 2887 cm^{-1}.

Cytotoxicity assay

The cytotoxicity of 5-ALA, HGNs, and conjugate was assessed after a 4-hour incubation time. An increase in 5-ALA concentration resulted in a marked enhancement of cell proliferation, with a significant difference noted between the control group and the group treated with 4 mM 5-ALA ($P<0.05$) (Fig. 3). However, no significant differences were observed between the various drug concentration groups in the other two groups.

Table 1. Physical characteristics of HGN_s and HGNS-PEG (17)

Nanoparticle	Size(nm)	Zeta-potential	PDI	Conductivity (mS/cm)
HGNS	43±2.21	-24±1.34	0.29±0.028	0.241±0.013
HGNS-PEG	58± 1.91	-19±1.9	0.25±0.022	0.007±0.001

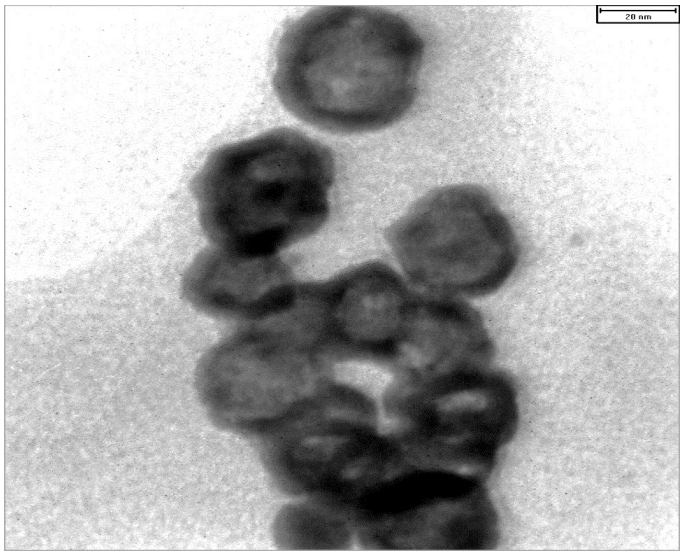

Fig. 1. TEM image of HGNS

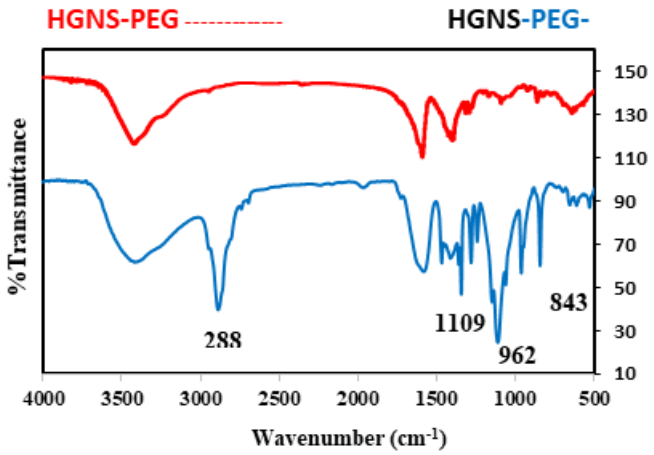

Fig. 2. conjugated of 5-ALA to HGNs

Treatment results

X-ray treatment

The radiosensitivity of each therapeutic agent was evaluated at specific concentrations, as determined during the cytotoxicity assessment. After incubating the drugs, X-ray treatments were performed at radiation doses of 2, 4, and 6 Gy across the four groups independently. In this research, the radiation sensitivity of therapeutic agents was investigated. The data indicate a significant difference between the control group and the groups that received the treatment dose, but there is no significant difference between all the groups that received different doses.

Photodynamic treatment

To evaluate the photosensitivity of the therapeutic agents, the agents were incubated for 4 hours with the KYSE 30 cell line. Following incubation, the cells were exposed to 630 nm light with 80 J/cm^2 for 1, 3, and 5 minutes. As shown in Figure 5(a, b) for 5-ALA and conjugate treatment groups, while there are significant differences between treated groups at various times (optical doses) for each concentration, no significant changes were observed between various concentrations of 5-ALA and conjugate. Notably, the conjugate treatment group exhibited a threefold enhancement in cell death rate compared to free

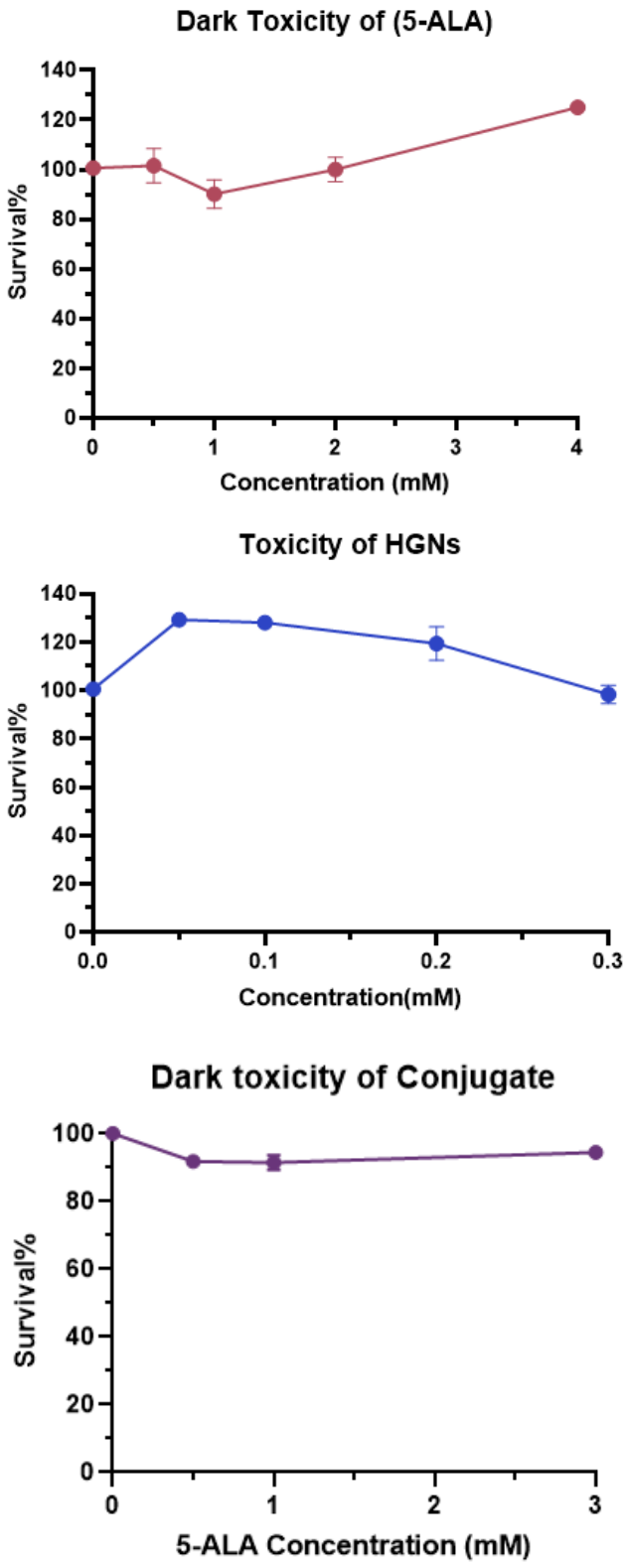

Fig. 3. a) Dark toxicity of different concentrations of 5-ALA b) Dark toxicity of various concentrations of HGN_s c) Dark toxicity of conjugate in the presence of various concentrations of 5-ALA in KYSE cells. Incubation time: 4 hours

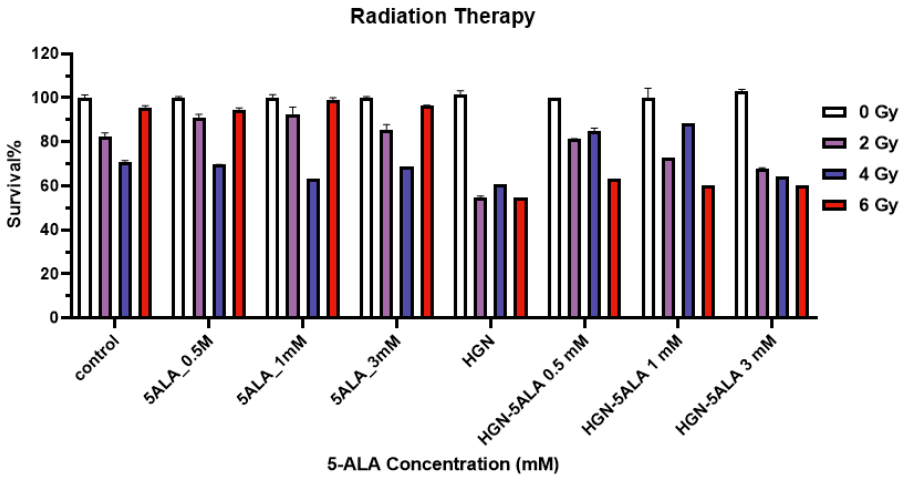

Fig. 4. Cell survival percentage control, 5-ALA, HGN_S and conjugate groups under various X-ray doses (RT), assessed 24 hours post-treatment with the KYSE 30 cell line. Data are presented as the mean ± standard error of the mean from three replicates.

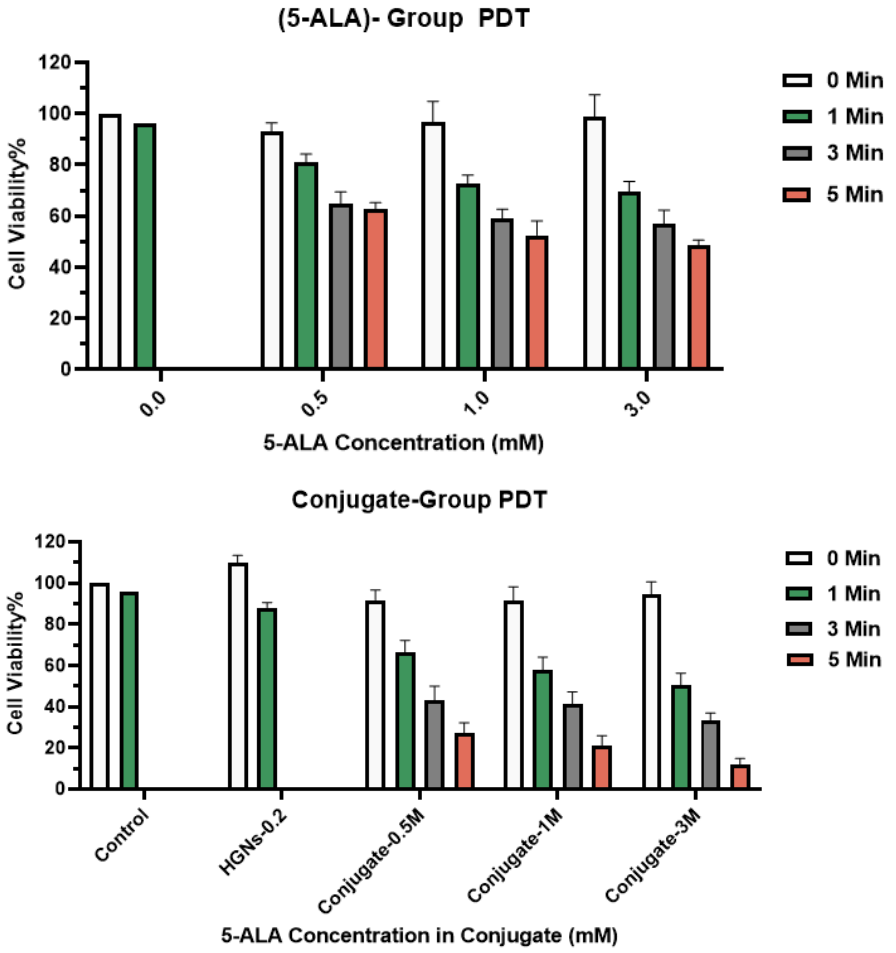

Fig. 5. (a, b) Phototoxicity (PDT) in KYSE cells after incubating for 4 hours with different concentrations of 5-ALAand conjugate in the dark and irradiation with 80 J/cm^2 for 0, 1, 3 and, 5 min. Data are presented as the mean ± standard error of the mean from three replicates.

5-ALA.

Figure 5b demonstrates that the synthesis and application of HGN_S as a 5-ALA drug carrier in PDT achieved an approximate lethality rate of 90%.

DISCUSSION

Squamous-cell carcinoma constitutes about 85% of deaths related to esophageal cancer (18). Despite treatments like chemotherapy, radiotherapy, and surgery, many patients ultimately need salvage and palliative therapies. The combination of 5-ALA and HGNs may enhance the effectiveness of both radiotherapy and PDT. With the advent of the second generation of photosensitizers and the enhanced tumor targeting and treatment efficacy enabled by nanostructures, this study explores the conjugation of 5-ALA with HGNs in RT and PDT to effectively treat KYSE carcinoma cells (4).

HGNs-PEG was synthesized with 43 nm of size by DLS measurement in this study. The FTIR mechanism relies on the excitation of molecules to higher vibrational states as a result of absorbing infrared (IR) radiation by the final nanostructure. By comparing the wavelengths absorbed by the final sample compared to the initial sample, the molecular structure of the new nanostructure can be more comprehensively understood. In this study, the FTIR technique was utilized to investigate the presence or absence of chemical bonds between 5-ALA molecules and HGNs. The comparative results of the FTIR test show that the bonding process of 5-ALA to the pegylated HGNs caused peaks in the numbers 843, 962, 1109, and 2887 cm-1 It can be concluded that the conjugation of 5-ALA with the surface of HGNs was successfully achieved. In this study, the cytotoxicity of the therapeutic agents was evaluated at four different. Other studies, such as those conducted by Wei Li et al. (19), reported no significant dark cytotoxicity in the incubation of HGNs (8 nm) with SKOV 3, CT-26, and B16 cell lines. In agreement with them, HGNs (10 nm) showed no significant effect on KYSE cell proliferation. Based on Fratoddi et al. (20), reported spherical nanopartilcles with sizes between 15 and 50 nm are less toxic. There is also no significant cytotoxicity report of 5-ALA up to 4 mM in esophageal and other types of cell lines in the literature (11, 21, 22). Our data indicated that conjugate did not also exhibit significant dark cytotoxicity.

In RT assessment, increasing the 5-ALA concentration up to 3 mM does not affect the treatment efficiency of RT (23). Unlike 5-ALA and its conjugate, HGNs alone effectively reduced KYSE cell viability following RT. There is evidence for the mediation of these nanostructures as radiosensitizers in several studies. Ionization of water molecules via X-ray absorption by PEG-HGNs, formation of hydroxyl radicals, and auger electron projection elevate DNA damage and protein deconstruction. PEGylation also assists in the elongated circulation and targeted delivery of HGNs. They exhibit photothermal ablation in addition to the other properties of tumor cell killing promotion (24, 25). The vital properties of gold nanostructures, including high LSPR and beneficial fluorescence quenching, in addition to their tendency to attach with disulfides, thiols, and amins, can raise their tumor cell influence (26). In none of the present or previous studies, 5-ALA did not act as a radiosensitizer in the presence of HGNs or HGNs (21). The incubation time after RT and the X-ray dosage were equal in both studies, and the size of HGNs (~10 nm) was smaller than that of HGNs (~34 nm). It is conceivable that the conjugated form diminished the fluorescence quenching of nanocarriers. According to the last studies, it seems that enhanced activation of growth factor signaling pathways and dysregulated miRNA contribute to damage to DNA, arrest the cell cycle, angiogenesis, and apoptosis, and are effective in radio-resistance of cancer cells (27, 28). Schaffer et al. also assume that some parameters, such as oxygen supply and improper cell cycle state, are impressive in the radioresistance potential of photosensitizers(29) .

In PDT, the present of conjugate treatment group showed a threefold increase in cell death rate compared to free 5-ALA alone and resulted in an approximate lethality rate of 90%. The synergistic effect observed in the conjugated group is related to the presence of HGNs within the nanostructure. Similar to conventional gold nanostructures, HGNs exhibit considerable potential for biomedical applications owing to their chemical stability, biocompatibility, and ease of surface modification. However, the most notable distinction between solid and HGNs is the presence of an internal cavity. The internal cavity imparts enhanced functionalities to HGNs, including the capacity for anticancer drug loading and the potential for interactions between the inner and outer surfaces. The large surface area of HGNs allow them to be

easily functionalized with photosensitizers, which are molecules that generate singlet oxygen or ROS upon light exposure. These can be loaded either on the surface of the HGNs or within the hollow core. HGNs heat can improve the uptake of the photosensitizer into cancer cells(30-32).

ACKNOWLEDGMENT

The data presented in this report was part of a research project in the department of medical physics, which was supported by the research deputy Babol University of Medical Sciences and Mashhad University of Medical Sciences.

CONFLICT OF INTEREST

The authors declare that there are no conflicts of interest.

REFERENCES

1. Nishikawa M, Yamamoto Y, Kushida S, Hirabayashi T, Tanaka S, Takegawa N, et al. Assessment of PDT as a salvage treatment for local failure after chemoradiotherapy or radiotherapy for esophageal cancer in patients aged 80 years or older. DEN open. 2023;3(1):e167. https://doi.org/10.1002/deo2.167
2. Thariat J, Hannoun-Levi J-M, Sun Myint A, Vuong T, Gérard J-P. Past, present, and future of radiotherapy for the benefit of patients. Nature reviews Clinical oncology. 2013;10(1):52-60. https://doi.org/10.1038/nrclinonc.2012.203
3. Mazraedoost S, Behbudi G. Nano materials-based devices by PDT for treating cancer applications. Advances in Applied NanoBio-Technologies. 2021;2(3):9-21.
4. Wu H, Minamide T, Yano T. Role of PDT in the treatment of esophageal cancer. Digestive Endoscopy. 2019;31(5):508-16. https://doi.org/10.1111/den.13353
5. Turkoglu EB, Rao R, Celik E. Long term outcome of adjuvant PDT after cyberknife radiotherapy for choroidal melanoma. Photodiagnosis and PDT. 2022;38:102840. https://doi.org/10.1016/j.pdpdt.2022.102840
6. Shinoda Y, Kato D, Ando R, Endo H, Takahashi T, Tsuneoka Y, et al. Systematic review and meta-analysis of in vitro anti-human cancer experiments investigating the use of 5-aminolevulinic acid (5-ALA) for PDT. Pharmaceuticals. 2021;14(3):229. https://doi.org/10.3390/ph14030229
7. Sobhani N, Sazgarnia A, Rajabi O, Soudmand S, Naghavi N. A study on the photobleaching effect of 5-ALA conjugated gold nanoparticles in a CT26 tumor model during PDT. 2012.
8. Mahmoudi K, Garvey K, Bouras A, Cramer G, Stepp H, Jesu Raj J, et al. 5-aminolevulinic acid PDT for the treatment of high-grade gliomas. Journal of neuro-oncology. 2019;141:595-607. https://doi.org/10.1007/s11060-019-03103-4
9. Kou J, Dou D, Yang L. Porphyrin photosensitizers in PDT and its applications. Oncotarget. 2017;8(46):81591. https://doi.org/10.18632/oncotarget.20189
10. Zhao R, Xiang J, Wang B, Chen L, Tan S. Recent advances in the development of noble metal NPs for cancer therapy. Bioinorganic Chemistry and Applications. 2022;2022. https://doi.org/10.1155/2022/2444516
11. Mohammadi Z, Sazgarnia A, Rajabi O, Soudmand S, Esmaily H, Sadeghi HR. An in vitro study on the photosensitivity of 5-aminolevulinic acid conjugated gold nanoparticles. Photodiagnosis and PDT. 2013;10(4):382-8. https://doi.org/10.1016/j.pdpdt.2013.03.010
12. Singh P, Pandit S, Mokkapati V, Garg A, Ravikumar V, Mijakovic I. Gold nanoparticles in diagnostics and therapeutics for human cancer. International journal of molecular sciences. 2018;19(7):1979. https://doi.org/10.3390/ijms19071979
13. Tiwari P, Bawage S, Singh S. Gold nanoparticles and their applications in photomedicine, diagnosis and therapy. Applications of Nanoscience in Photomedicine: Elsevier; 2015. p. 249-66. https://doi.org/10.1533/9781908818782.249
14. Adams S, Zhang JZ. Unique optical properties and applications of hollow gold nanospheres (HGNs). Coordination Chemistry Reviews. 2016;320:18-37. https://doi.org/10.1016/j.ccr.2016.01.014
15. Li Y, He D, Tu J, Wang R, Zu C, Chen Y, et al. The comparative effect of wrapping solid gold nanoparticles and hollow gold nanoparticles with doxorubicin-loaded thermosensitive liposomes for cancer thermo-chemotherapy. Nanoscale. 2018;10(18):8628-41. https://doi.org/10.1039/C7NR09083H
16. Miao Z, Gao Z, Chen R, Yu X, Su Z, Wei G. Surface-bioengineered gold nanoparticles for biomedical applications. Current Medicinal Chemistry. 2018;25(16):1920-44. https://doi.org/10.2174/0929867325666180117111404
17. Imanparast A, Attaran N, Sazgarnia A. In Vitro Investigation into Plasmonic Photothermal Effect of Hollow Gold Nanoshell Irradiated with Incoherent Light. Iranian Journal of Medical Physics. 2018;15(3):161-8.
18. Arnold M, Ferlay J, van Berge Henegouwen MI, Soerjomataram I. Global burden of oesophageal and gastric cancer by histology and subsite in 2018. Gut. 2020;69(9):1564-71. https://doi.org/10.1136/gutjnl-2020-321600
19. Li W, Zhang H, Guo X, Wang Z, Kong F, Luo L, et al. Gold nanospheres-stabilized indocyanine green as a synchronous photodynamic-photothermal therapy platform that inhibits tumor growth and metastasis. ACS applied materials & interfaces. 2017;9(4):3354-67. https://doi.org/10.1021/acsami.6b13351
20. Fratoddi I, Venditti I, Cametti C, Russo MV. How toxic are gold nanoparticles? The state-of-the-art. Nano Research. 2015;8:1771-99. https://doi.org/10.1007/s12274-014-0697-3
21. Mohammadi Z, Sazgarnia A, Rajabi O, Seilanian Toosi M. Comparative study of X-ray treatment and PDT by using 5-aminolevulinic acid conjugated gold nanoparticles in a melanoma cell line. Artificial Cells, Nanomedicine, and Biotechnology. 2017;45(3):467-73. https://doi.org/10.3109/21691401.2016.1167697
22. Chen X, Zhao P, Chen F, Li L, Luo R. Effect and mechanism of 5-aminolevulinic acid-mediated PDT in esophageal cancer. Lasers in medical science. 2011;26:69-78. https://doi.org/10.1007/s10103-010-0810-0
23. Shishido Y, Amisaki M, Matsumi Y, Yakura H, Nakayama Y, Miyauchi W, et al. Antitumor effect of 5-aminolevulinic acid through ferroptosis in esophageal squamous cell carcinoma. Annals of Surgical Oncology. 2021;28:3996-

4006. https://doi.org/10.1245/s10434-020-09334-4
24. Wang R, Deng J, He D, Yang E, Yang W, Shi D, et al. PEGylated hollow gold nanoparticles for combined X-ray radiation and photothermal therapy in vitro and enhanced CT imaging in vivo. Nanomedicine: Nanotechnology, Biology and Medicine. 2019;16:195-205. https://doi.org/10.1016/j.nano.2018.12.005
25. Shen Y, Xia Y, Yang E, Ye Z, Ding Y, Tu J, et al. A polyoxyethylene sorbitan oleate modified hollow gold nanoparticle system to escape macrophage phagocytosis designed for triple combination lung cancer therapy via LDL-R mediated endocytosis. Drug Delivery. 2020;27(1):1342-59. https://doi.org/10.1080/10717544.2020.1822459
26. Nejati K, Dadashpour M, Gharibi T, Mellatyar H, Akbarzadeh A. Biomedical applications of functionalized gold nanoparticles: a review. Journal of Cluster Science. 2021:1-16. https://doi.org/10.1007/s10876-020-01955-9
27. Malhotra A, Sharma U, Puhan S, Bandari NC, Kharb A, Arifa P, et al. Stabilization of miRNAs in esophageal cancer contributes to radioresistance and limits efficacy of therapy. Biochimie. 2019;156:148-57. https://doi.org/10.1016/j.biochi.2018.10.006
28. Rho O, Kim DJ, Kiguchi K, DiGiovanni J. Growth factor signaling pathways as targets for prevention of epithelial carcinogenesis. Molecular carcinogenesis. 2011;50(4):264-79. https://doi.org/10.1002/mc.20665
29. Schaffer M, Ertl-Wagner B, Schaffer Pa, Kulka U, Jori G, Duhmke E, et al. The application of photofrin II® as a sensitizing agent for ionizing radiation-a new approach in tumor therapy? Current medicinal chemistry. 2005;12(10):1209-15. https://doi.org/10.2174/0929867053764653
30. Park J-M, Choi HE, Kudaibergen D, Kim J-H, Kim KS. Recent advances in hollow gold nanostructures for biomedical applications. Frontiers in Chemistry. 2021;9:699284. https://doi.org/10.3389/fchem.2021.699284
31. Yang Y, Zheng X, Chen L, Gong X, Yang H, Duan X, et al. Multifunctional gold nanoparticles in cancer diagnosis and treatment. International journal of nanomedicine. 2022:2041-67. https://doi.org/10.2147/IJN.S355142
32. Mohseni H, Imanparast A, Salarabadi SS, Sazgarnia A. In vitro evaluation of the intensifying photodynamic effect due to the presence of plasmonic hollow gold nanoshells loaded with methylene blue on breast and melanoma cancer cells. Photodiagnosis and PDT. 2022;40:103065. https://doi.org/10.1016/j.pdpdt.2022.103065